# Electrochemical Studies of the Inhibition Effect of 2-Dimethylaminoethanol on the Corrosion of Austenitic Stainless Steel Type 304 in Dilute Hydrochloric Acid

## Roland T. Loto, Cleophas A. Loto, Abimbola P. Popoola & Tatiana Fedotova

Springer

Springer

CrossMark

ORIGINAL PAPER

# Electrochemical Studies of the Inhibition Effect of 2-Dimethylaminoethanol on the Corrosion of Austenitic Stainless Steel Type 304 in Dilute Hydrochloric Acid
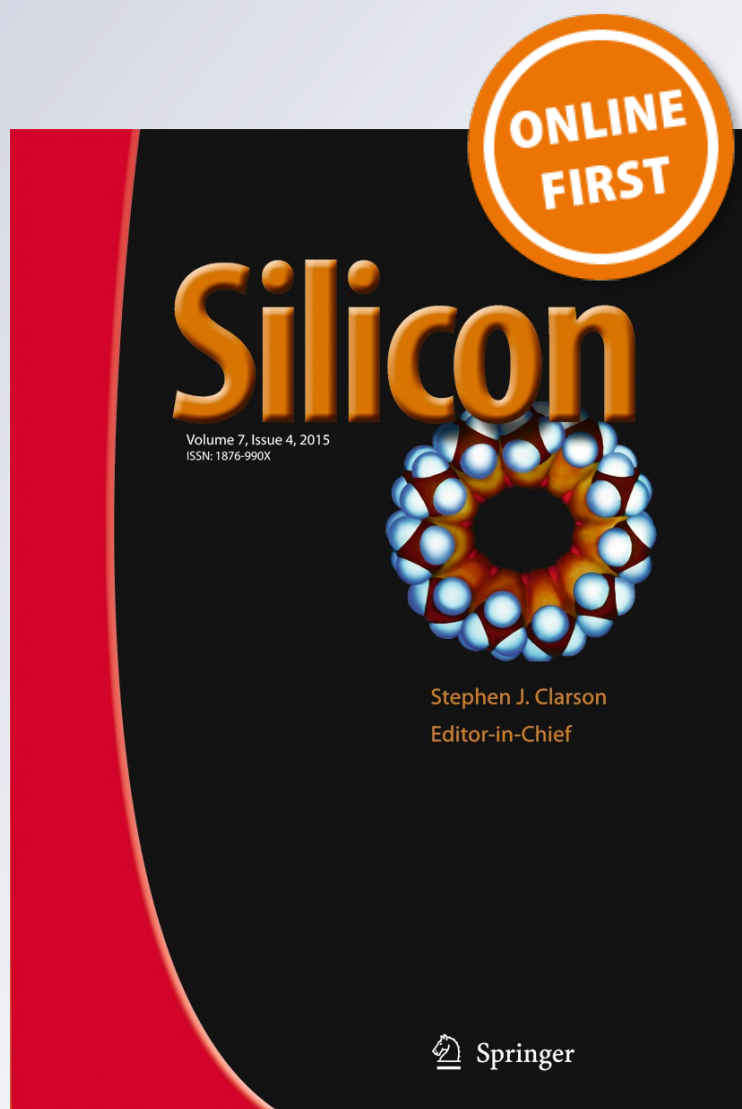
Roland T. Loto[1,2] · Cleophas A. Loto[1,2] · Abimbola P. Popoola[2] ·
Tatiana Fedotova[2]

**Abstract** The electrochemical behaviour of 2-dimethyl-aminoethanol (DMA) on the corrosion of Type 304 austenitic stainless steel in dilute hydrochloric solution was investigated through a weight-loss technique, open circuit potential measurement and potentiodynamic polarization tests at specific concentrations of DMA. Results show the compound to be highly effective with a maximum inhibition efficiency of 79 % from weight loss analyses and 80.9 % from polarization tests at 12.5 % DMA. The mean corrosion potential of −321 mV, obtained from open circuit potential measurement is within passivation potentials. DMA inhibition protection was determined to occur through a physicochemical reaction mechanism on the steel surface, confirmed from calculated thermodynamic values. DMA obeyed the Langmuir isotherm model. Data obtained for inhibition efficiency from the three test techniques are in reasonably good agreement. The potentiodynamic test showed that the compounds acted as a cathodic type inhibitor.

✉ Roland T. Loto
tolu.loto@gmail.com

1  Department of Mechanical Engineering, Covenant University, Ota, Ogun State, Nigeria

2  Department of Chemical, Metallurgical & Materials Engineering, Tshwane University of Technology, Pretoria, South Africa

## 1 Introduction

Functional surfaces, functional films, and surface coatings have become important subjects in recent technologies [1–4]. Especially, protection of surfaces of materials against corrosion by some chemicals such as hydrochloric acid is crucial. Hydrochloric acid is extensively applied in industry in areas such as pickling of ferrous alloys, industrial processing, mining and extraction, petroleum refinery and oil well acidizing [5]. These applications involve the use of ferrous alloys especially steel and are affected by their corrosion and the consequent cost of maintenance. Application of corrosion inhibitors is a versatile and economical technique for corrosion control in acidic media. Studies have shown that inhibitor adsorption on metallic surfaces is subject to the physicochemical characteristics of inhibitor molecules such as functional groups, steric factors, aromacity, electron density of the donor atoms, polymerization resulting in formation of protective films and the electronic structure of the molecules [6–8]. A significant number of corrosion inhibitors in service are organic compounds [9–15]. Organic compounds consisting of functional groups with heteroatoms such as oxygen, nitrogen and sulfur capable of donating valence electrons, have been observed to perform excellently against metallic corrosion in a significant number of industrial conditions [16–18].

Some publications focussed on the extensive application of acetylenic alcohols such as propargyl alcohol as inhibitors in hydrochloric acid media. Industrially acetylenic alcohols are used as effective inhibitors for acid descaling and pickling of stainless steel [19–29]. The importance of the triple bonds of acetylenic alcohol molecules which is the result of interaction of pi-electrons with the alloy interface has been confirmed. The corrosion inhibition

Springer

behaviour of 2-butyn-1-ol on austenitic stainless steel and 2-butyne 1-4 diol on low carbon steel in sulfuric acid media was observed to be effective [22–25, 27, 30]. Amino alcohols have been investigated for their corrosion behaviour on reinforcing steel due to their penetration ability [31–37]. Machnikova et al. and Vaidyanathan and Hackerman studied the inhibition effect of 2-methylfuran, furfuryl alcohol and furfurylamine on carbon steel in hydrochloric acid [38, 39]. A number of environmentally friendly organic compounds containing polar functions with nitrogen, oxygen, and/or sulfur in conjugated systems in their molecules have been well applied as inhibiting agents in harsh industrial conditions [40–47]. The inhibiting action of such compounds is attributed to the adsorption of the additives to the metal/solution interface. In continuation of the research on organic derivatives, this research focuses on the corrosion inhibition effect of 2-dimethylaminoethanol at specific concentrations in dilute HCl test solutions using linear polarization, weight loss techniques and open circuit potential measurements.

## 2 Experimental Procedure

### 2.1 Material

Type 304 austenitic stainless steel obtained commercially was used for all experimentation . The Energy Dispersive Spectroscopy analysis using a Jeol JSM - 7600F UHR Analytical FEG SEM, and a state of- the-art Ultra-High Resolution Analytical Thermal Field Emission Gun Scanning Electron Microscope from Electrochemical & Materials Characterization Research Laboratory, Department of Chemical, Metallurgical Engineering and Materials Engineering, Tshwane University of Technology, Pretoria, South Africa gave the general nominal composition of 18.11 % Cr, 8.32 % Ni and 68.32 % Fe. The steel has a cylindrical dimension of 18 mm diameter.

### 2.2 Inhibitor

2-dimethylaminoethanol (DMA), a colorless, transparent organic chemical liquid, is the inhibitor used. The molecular formula is $C_4H_{11}NO$, while the molar mass is 89.14 $gmol^{-1}$. DMA was prepared in concentrations of 2.5 %, 5 %, 7.5 %, 10 %, 12.5 % and 15 %.

### 2.3 Test Media

3 M hydrochloric acid (HCl) with 3.5 % recrystallized sodium chloride (NaCl) of Analar grade was used as the corrosion test medium.

### 2.4 Preparation of Test Specimens

The stainless steel (18 mm dia.) was machined into a number of samples between 17.8 mm to 18.8 mm in length. The exposed surface ends of the samples were metallographically prepared with silicon carbide abrasive papers of 80, 120, 220, 800 and 1000 grits before being polished with diamond paste from 6.0 $\mu$m to 1.0 $\mu$m, washed with distilled water, rinsed with acetone, dried and stored in a dessicator for testing.

### 2.5 Weight-Loss Experiments

The weighed test samples were each immersed in 200 ml of the acid test solutions at specific concentrations of the DMA for 312 h at 25°C. The samples were monitored every 72 h after washing with deionised water, rinsing with acetone, drying and re-weighing. Graphical illustrations of weight-loss (mg) and corrosion rate (mm/y) versus exposure time (h) (Figs. 2 and 3) and those of percentage inhibition efficiency (*%IE*) (calculated) versus exposure time (h) and percentage DMA concentration (Figs. 3 and 4) were derived from Table 1.

The corrosion rate ($R$) is derived from Eq. 1:

$$R = \left[ \frac{87.6W}{DAT} \right] \tag{1}$$

Where $W$ is the weight loss (mg), $D$ is the density (g/cm$^2$), $A$ is the area in cm$^2$, and $T$ is the time (h) of exposure. The *%IE* was calculated from the mathematical relationship depicted in Eq. 2.

$$\%IE = \left[ \frac{R_1 - R_2}{R_1} \times 100 \right] \tag{2}$$

Where $R_1$ and $R_2$ are the corrosion rates with and without DMA concentrations. The *%IE* is determined for all the DMA concentrations at a 72 h interval during the experimental period while the surface coverage is determined from the relationship:

$$\theta = \left[ 1 - \frac{W2}{W1} \right] \tag{3}$$

Where $\theta$ is the amount of DMA inhibitor adsorbed per gram (or kg) of the adsorbent. $W_1$ and $W_2$ are the weight loss of the steel sample with and without DMA inhibited acid media respectively.

### 2.6 Open Circuit Potential Measurement

An electrochemical cell consisting of a two-electrode with Ag/AgCl as the reference electrode was used. The open circuit potential values (OCP) were obtained with an

**Table 1** Data obtained from weight loss measurements for austenitic stainless steel in 3 M HCl in presence of specific concentrations of the DMA at 312 h

| Sample | Inhibitor concentration (%) | Weight loss (mg) | Corrosion rate (mm/y) | Inhibition efficiency (%) |
|---|---|---|---|---|
| A | 0 | 2813 | 16.3374 | 0 |
| B | 2.5 | 1953 | 9.234 | 30.6 |
| C | 5 | 1471 | 7.4806 | 47.7 |
| D | 7.5 | 1221 | 4.6342 | 56.6 |
| E | 10 | 1043 | 4.1347 | 62.9 |
| F | 12.5 | 592 | 2.2613 | 79 |
| G | 15 | 593 | 2.1984 | 78.9 |

Autolab PGSTAT 30 ECO CHIMIE potentiostat. Resin mounted steel samples with an exposed surface area of 254 mm$^2$ were each immersed in 200 ml of the acid chloride solution at specific DMA concentrations for 288 h. The OCP of each steel sample was measured at a 48 h interval. Graphical illustrations of corrosion potential (mV) against immersion time (h) (Fig. 5) are obtained from the OCP data in Table 2.

### 2.7 Potentiodynamic Polarization

Potentiodynamic polarization tests were carried out using embedded steel samples in plastic mounts with an exposed surface area of 254 mm$^2$. The samples were metallographically prepared with different grits of abrasive silicon carbide paper, burnished to 6 $\mu$m, cleaned with deionized water and dried with acetone. The measurements were done at 25 °C with an Autolab PGSTAT 30 ECO CHIMIE potentiostat and electrode cell containing 200 ml of the acid solution, with and without the DMA compound. A graphite rod was applied as the auxiliary electrode and Ag/AgCl was the standard reference electrode. The potential was cursorily examined from -1.5V versus OCP to +1.5 mV versus OCP at a scan rate of 0.00166 V/s. The corrosion currents and current density were obtained. The corrosion current density

($i_{corr}$) and corrosion potential ($E_{corr}$) were determined from the Tafel plots of potential versus log $I_{corr}$. The corrosion rate ($R$), the degree of surface coverage ($\theta$) and the percentage inhibition efficiency (%IE) were calculated as follows

$$R = \frac{0.00327 \times I_{corr} \times E_q}{D} \qquad (4)$$

where $I_{corr}$ is the current density ($\mu$A/cm$^2$), D is the density (g/cm$^3$); $E$q is the specimen equivalent weight (g);

The percentage inhibition efficiency (%IE) was determined from the corrosion current density values from Eq. 5.

$$\%IE = 1 - \left[ \frac{R_2}{R_1 \times 100} \right] \qquad (5)$$

where $R_1$ and $R_2$ are the corrosion current densities in the absence and presence of inhibitors, respectively.

### 2.8 Scanning Electron Microscopy Characterization

The electron micrographs of the surface topography of the uninhibited and inhibited stainless steel surfaces were obtained and studied after weight-loss analysis with the aid of a Jeol scanning electron microscope.

### 2.9 X-Ray Diffraction Analysis

X-ray diffraction (XRD) patterns of the film formed on the metal surface with and without DMA addition were analyzed using a Bruker AXS D2 phaser desktop powder diffractometer with monochromatic Cu K$\alpha$ radiation produced at 30 kV and 10 mA, with a step size of 0.03°2$\theta$. The measurement program is the general scan xcelerator.

### 2.10 Statistical Analysis

Two-factor single level statistical analysis using the ANOVA test ($F$-test) was used to determine the statistical significance of DMA concentration and exposure time on the inhibition efficiency values of the DMA in the acid solution.

**Table 2** Data obtained from potential measurements for austenitic stainless steel in 3 M HCl in presence of specific concentrations of the DMA

| DMA concentration (%) Exposure time (h) | 0% | 2.5 % | 5 % | 7.5 % | 10 % | 12.5 % | 15 % |
|---|---|---|---|---|---|---|---|
| 0 | −497 | −393 | −321 | −340 | −359 | −363 | −380 |
| 48 | −482 | −374 | −318 | −326 | −324 | −334 | −349 |
| 96 | −487 | −369 | −313 | −321 | −322 | −331 | −335 |
| 144 | −490 | −352 | −316 | −323 | −323 | −324 | −330 |
| 192 | −498 | −341 | −321 | −325 | −324 | −324 | −326 |
| 240 | −502 | −327 | −320 | −324 | −322 | −321 | −324 |
| 288 | −497 | −325 | −318 | −321 | −320 | −321 | −322 |

**Fig. 1** Variation of weight-loss with exposure time for samples (A – G) in (0 % –15 %) DMA concentrations in 3 M HCl
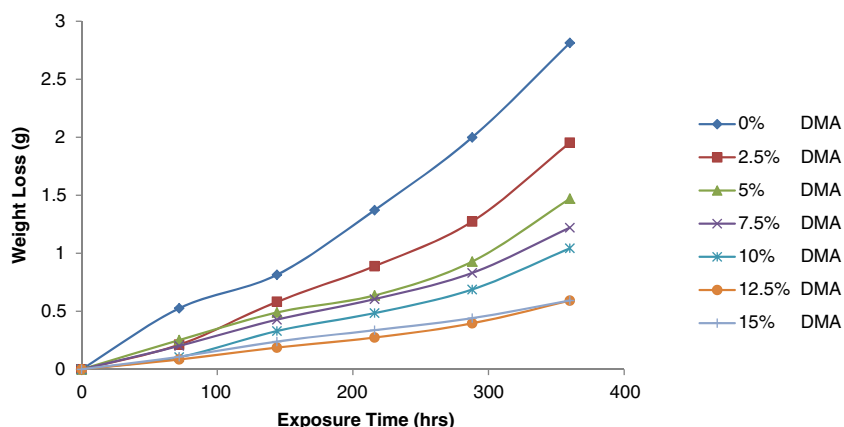


## 3 Results and Discussion

### 3.1 Weight-Loss Analysis

The weight-loss of the stainless steel with and without DMA addition at specific concentrations was studied in 3 M HCl. The data from weight-loss ($W$), corrosion rate ($R$) and the percentage inhibition efficiency (%IE) are tabulated in Table 1. Observation shows that decrease in corrosion rate corresponds with increase in DMA concentration. This shows that more DMA molecules are adsorbed onto the alloy surface, resulting in more effective surface coverage of the steel. Figures 1, 2 and 3 show the graphical illustration of weight-loss, corrosion rate and percentage inhibition efficiency versus exposure time at specific DMA concentrations while Fig. 4 shows the plots of %IE with inhibitor concentration. The plots show a progressive increase in %IE with increase in DMA concentration accompanied by a significant decrease in corrosion rate.

As DMA concentration increases the steel surface becomes more passivated due to the changes in the electrochemical reactions within the test solution whereby the reactive sites on the specimen surface are totally separated from the acid chloride solution. DMA forms a compact barrier or film which prevents the diffusion of $Fe^{2+}$ to the liquid/metal interface while at the same time it inhibits the diffusion of chloride ions to the metal/liquid interface. The barrier becomes more effective as the number of DMA molecules increases preventing dissolution of the steel specimens.

The barrier film is strongly adsorbed through physico-chemical mechanisms, thus it is chemically bonded onto the surface of the steel. This film remains virtually intact during the exposure period. The influence of DMA on the electrochemical reactions in 3 M HCl is highly significant as shown in the plots of the various concentrations from 2.5 % - 15 %. The values of %IE in Table 1 attest to these observations. %IE values in Table 1 vary from 30.6 % to 78.9 %, thus it can be deduced that DMA is effective in 3 M HCl from 10 % concentration upward.

### 3.2 Open Circuit Potential Measurement

The open-circuit potential values of the specimen electrodes were observed for a total of 288 h in the acid chloride solutions as shown in Table 2, generally the equilibrium state was reached within 60 min. Figure 5 depicts the variation of open-circuit potentials with time in 3 M HCl chloride solutions respectively in the absence and presence of specific concentrations of DMA compound. Analysis of the control

**Fig. 2** Effect of percentage concentration of DMA on the corrosion rate of austenitic stainless steel in 3 M HCl
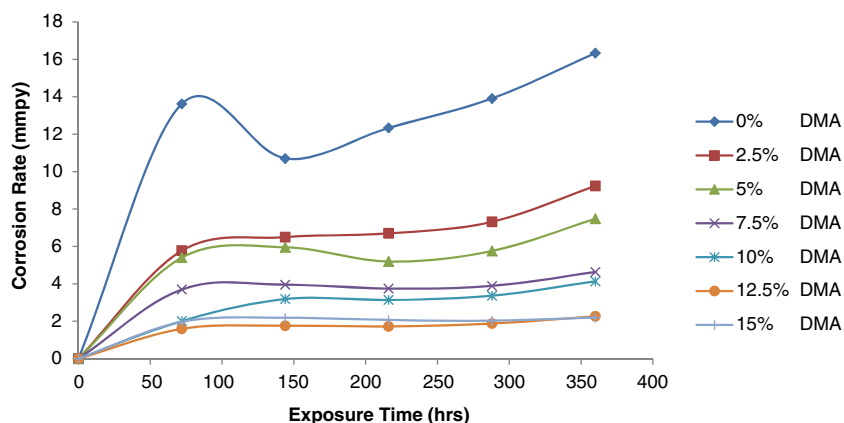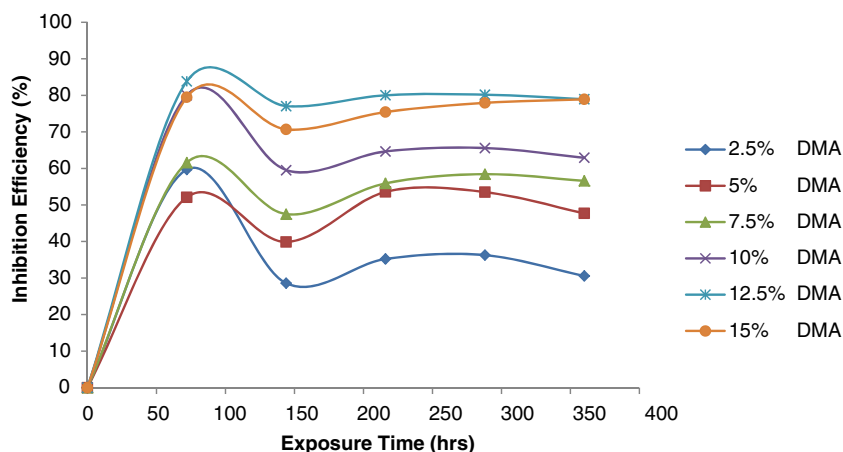
**Fig. 3** Plot of inhibition efficiencies of sample (A-G) versus exposure time in 3 M HCl during the exposure period



specimen (0 % DMA, Table 2) reveals the corrosive nature of the hydrochloric acid solution. The potential values progressed significantly towards more negative potentials, an indication that anodic dissolution is actively taking place in the absence of DMA which results in alloy degradation and formation of corrosion products including oxides on the specimen surface.

The potential values of 2.5 % - 15 % DMA concentration generally remained in a steady state throughout the immersion period from slight positive displacements of the potential values in the first 50 h. With the exception of 0 % DMA concentration results reveal the surface of the stainless steel to be electrochemically stable in hydrochloric acid due to the increased stability of the protective film of DMA whereby an average value of between -320 mV and -330 mV is maintained throughout. The potential shift towards more negative values at 0 % DMA in the acid indicates the enhancement of the steel's corrosion susceptibility in the absence of DMA, due to adsorption of the chloride ions onto the steel surface during the electrochemical process. This electrolytic action maintains the potential values in the

domain of active corrosion reaction resulting in uniform and pitting corrosion failure of the steel specimen.

Most pits initiate and grow at inclusion sites and structural defects on the steel surface which results in active metal dissolution, but increase in potential results in a condition where the electrochemical reactions are responsible for the formation of oxide thermodynamically. The effective surface for alloy deterioration reduces and passivation occurs when the entire surface is covered by the DMA film. In the presence of DMA competitive adsorption exists between the inhibitor and the aggressive anions as shown in the displacement of the potential results to more noble/ stable values within the passive domain. In effect the ability of DMA to inhibit corrosion improves with time which is a positive indication of its inhibitive nature

### 3.3 Polarization Studies

The electrochemical effect of the addition of DMA inhibitor on the polarization plots of Type 304 stainless steel in 3 M

**Fig. 4** Variation of Inhibition efficiency of DMA versus DMA concentrations from weight loss analysis in 3 M HCl
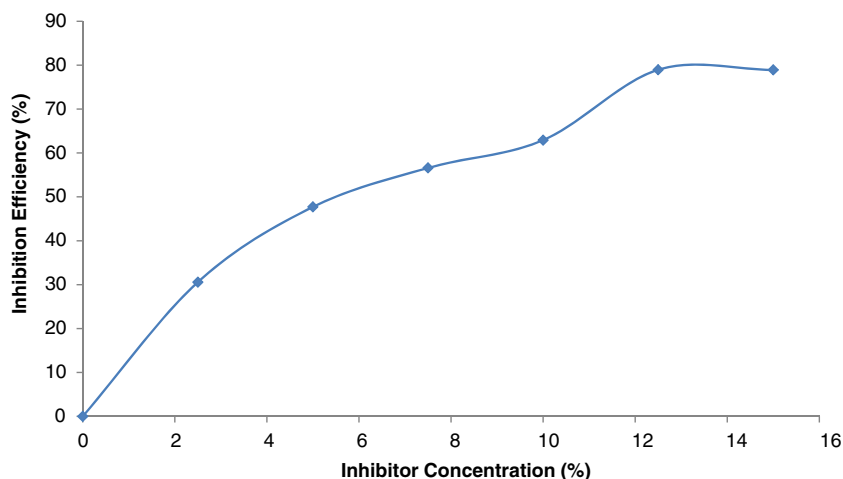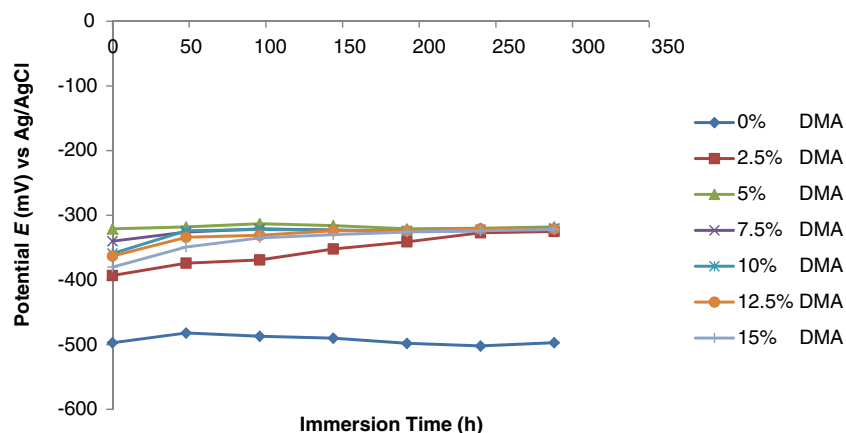
**Fig. 5** Variation of potential with immersion time for potential measurements in 3 M HCl



HCl solutions at 25 °C was studied. Figure 6 illustrates the potentiodynamic polarization curves depicting the relationship of the logarithm of current density $I$ (mAcm$^{-2}$) with the scanned applied potential $E$ (mV) versus the working electrode for DMA in 3 M HCl. The adsorption of DMA is subject to the value of its concentrations in the acid solutions as shown in Fig. 7; increase in DMA concentration results in a substantive increase in inhibition efficiency due to the availability of more DMA molecules to counteract the actions of the corrosive species, block the active sites and form a compact protective barrier on the alloy surface [48, 49]. Results obtained using Tafel and linear polarization methods indicate that adsorbed DMA compound on the surface of the metal electrode retarded the electrochemical process of corrosion. Anodic and cathodic currents were significantly influenced with increasing concentrations of DMA.

In Fig. 6 the corrosion potential shifts towards more positive potentials as DMA concentration increases, thus passivating iron through adsorption This also can be attributed to deposition of DMA cations on the alloy as a result of interaction between the inhibitor and the oxidized metal surface which effectively seals the surface against further reaction; however the cathodic process predominates over the anodic. The polarization scans are generally similar until

12.5 % - 15 % where there is a significant change due to the passivating action of the inhibitor. The results generally show that the %IE increased while the corrosion rates reduced.

Corrosion potential ($E_{cr}$), corrosion current ($i_{cr}$), corrosion current density ($I_{cr}$), cathodic Tafel constant ($b_c$), anodic Tafel slope ($b_a$) , surface coverage ($\theta$) and inhibition efficiency (%IE) values were determined and are shown in Table 3. The corrosion current density ($I_{cr}$) and corrosion potential ($E_{cr}$) were calculated from the intersection of the extrapolated anodic and cathodic Tafel plots, inhibition efficiency %IE was determined from the equation below

$$\%IE = \frac{R_1 - R_2}{R_1}\%  \qquad (6)$$

Table 3 shows results where the compound displayed a greater tendency for cathodic inhibition as observed in the displacement direction of the $E_{corr}$ values. This observation proves that DMA influences the cathodic reaction mechanism (hydrogen evolution and oxygen reduction) catalytically. The addition of DMA stifles the reaction. The molecular structure of DMA shows it might be able to adsorb on the metal surface through nitrogen atoms when protonized in the acid media.

**Fig. 6** Comparison plot of cathodic and anodic polarization scans for austenitic stainless steel in 3 M HCl + 3.5 % NaCl solution in the absence and presence of (0 % - 15 %) DMA
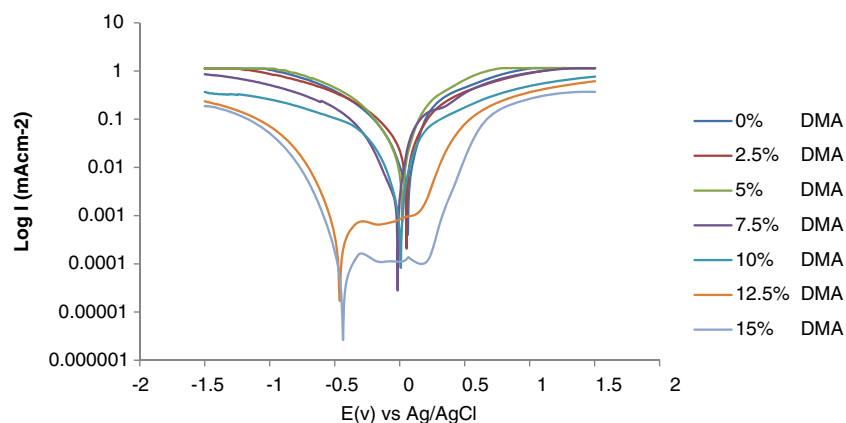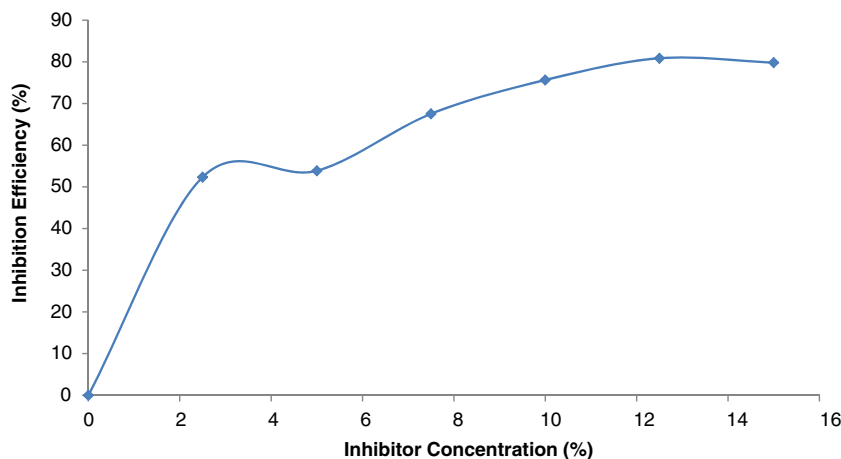
**Fig. 7** Relationship between *%IE* and inhibitor concentration for polarization test in 3 M HCl



Moreover, the presence of the hydroxyl group in the compound increases its solubility in the electrolytic media. In both solutions results show that the inhibition mode of the DMA is by surface coverage via film formation. The increase in the number of adsorbed DMA molecules on the steel is proportional to the increase in the percentage increase in DMA concentration. This mechanism obstructs the electrolytic transport of ionic species (chlorides and sulfates) from the electrode surface as the surface coverage ($\theta$) increases. The adsorption blocks the reaction sites of the metal surface thus affecting the anodic reaction mechanism.

Corrosion potentials slightly shifted in the negative direction in HCl. In this study the maximum displacement in $E_{corr}$ value is -188 mV in HCl, thus in HCl DMA is a cathodic type inhibitor. Slight deviation in corrosion potentials is most probably due to competition between the anodic and the cathodic inhibiting reactions. DMA acts more on the cathodic sites in 3 M HCl minimizing the rate of corrosion causing a significant change in corrosion potential. The hydrogen evolution reaction is inhibited and this increases with increase in DMA values. The variable nature of the cathodic slope (Fig. 6) also indicates that the mechanism of protonation changes with addition of the DMA to the acidic solution. In Fig. 6 there is a significant displacement of the corrosion potential between 0 % and 10 % DMA concentration due to the influence of cathodic reactions. At 12.5 % to

15 % passivation occurs at ∼352 mV to between ∼86 mV and 143 mV delaying the formation of pits.

### 3.4 Mechanism of Inhibition

Inhibition by DMA is the result of adsorption which depends on the inhomogeneities of the metal surface, type and condition of the electrolyte, the electrochemical reaction mechanism and its chemical structure. The physico-chemical characteristics of DMA are related to its functional groups and chemical reactivity. The interaction of pi-orbitals of DMA with d-orbitals of the surface atoms of the metal is responsible for the adsorption bond strength and the nature of the protective film. Adsorption of DMA is assumed to occur by two processes (a) electrostatic attraction between charged DMA molecules and the metal surface and (b) a chemical reaction mechanism due to charge transfer between the pi-electrons of the nitrogen atoms of the inhibitor molecules with vacant d-orbitals of the metal. The functional group responsible for DMA electrostatic adsorption on the metal surface is the hydroxyl ion through Van der Waals forces. The iron cations on the metal surface behave as a Lewis base due to reception of electrons from DMA [50–53].

DMA exists as cations in the acid media due to hydrogen, thus becoming highly reactive. The cation species

**Table 3** Data obtained from polarization resistance measurements for austenitic stainless steel in 3 M HCl in presence of specific concentrations of the DMA

| Inh. Conc. (%) | Corr. Rate (mm/yr) | % IE | $R_p$ ($\Omega$) | $E_{corr}$, Obs (V) | $E_{corr}$, Cal (V) | $i_{corr}$(A) | $I_{corr}$ (A/cm$^2$) | bc (V/dec) | ba (V/dec) |
|---|---|---|---|---|---|---|---|---|---|
| 0 | 6.61 | 0 | 6.04 | −0.313 | 0.062 | 1.47E-03 | 5.80E-04 | 0.031 | 0.060 |
| 2.5 | 3.15 | 52.3 | 13.62 | −0.422 | 0.052 | 7.01E-04 | 2.76E-04 | 0.034 | 0.062 |
| 5 | 3.05 | 53.9 | 15.45 | −0.322 | 0.019 | 6.79E-04 | 2.67E-04 | 0.052 | 0.045 |
| 7.5 | 2.15 | 67.5 | 21.65 | −0.313 | −0.016 | 4.78E-04 | 1.88E-04 | 0.201 | 0.027 |
| 10 | 1.61 | 75.6 | 25.76 | −0.342 | 0.009 | 3.58E-04 | 1.41E-04 | 0.048 | 0.038 |
| 12.5 | 1.27 | 80.9 | 23.21 | −0.496 | −0.460 | 2.83E-04 | 1.11E-04 | 0.044 | 0.023 |
| 15 | 1.33 | 79.8 | 35.65 | −0.501 | −0.435 | 2.95E-04 | 1.16E-04 | 0.046 | 0.051 |

adsorb on the cathodic sites suppressing the hydrogen evolution reaction while simultaneously adsorbing on the anodic sites thereby decreasing the anodic dissolution of the steel. This process is due to the donation of electrons from the nitrogen atoms resulting in electron sharing with the steel and formation of strong covalent bonds. Chloride ions are first absorbed onto the steel under the influence of high electric field through electrochemical diffusion onto the positively charged steel interface. This process results in the migration of DMA cations onto the steel to balance the polarities. The process in effect enables physical adsorption onto the steel due to the synergism between the chloride and DMA cations. A coordinate bond is also formed simultaneously by the transfer of electrons from nitrogen and oxygen atoms to the metal surface [54–56]. Alternatively it can be assumed that DMA displaces the chloride ions through competitive adsorption on the steel surface thereby keeping the passive film intact but this is unlikely, as from proven analysis DMA adsorption is physicochemical.

### 3.5 Scanning Electron Microscopy

The SEM images of the stainless steel surfaces before immersion in the acidic media in 3 M HCl solutions after 312 h immersion with and without inhibitor are given in Fig. 8a–d, respectively. Figure 8a & b shows the EDS analysis results and steel sample before immersion, the lined surface is due to cutting during preparation. Figure 8c shows the steel surfaces after 312 h of immersion in 3 M HCl without DMA, while Fig. 8d shows the steel surface in the acid media with DMA. In the absence of DMA, a very rough and porous surface is observed in Fig. 8c. Large numbers of micro-pits coupled with a badly corroded topography of the stainless steel coupons are visible as a result of the corrosive actions of chloride ions due to the breakdown of the passive film of chromium oxide as the high diffusivity of the chloride ions through cracks and the passive film is faster than the rate of repassivation.

The adsorption of the negatively charged chloride species on the stainless steel surface results in excess charge leading to cation (protonated DMA) adsorption on the steel surface. The protonated DMA molecules adsorb on the steel surface via a connecting bridge through the chloride ions responsible for the electrolytic diffusion of DMA onto the steel surface. Electrostatic interaction is believed to occur between the protonated molecules and the oxidized iron species at anodic sites, thus the significant morphological improvement on the surface of the stainless steel in the presence of DMA [57, 58] [Fig. 8d].
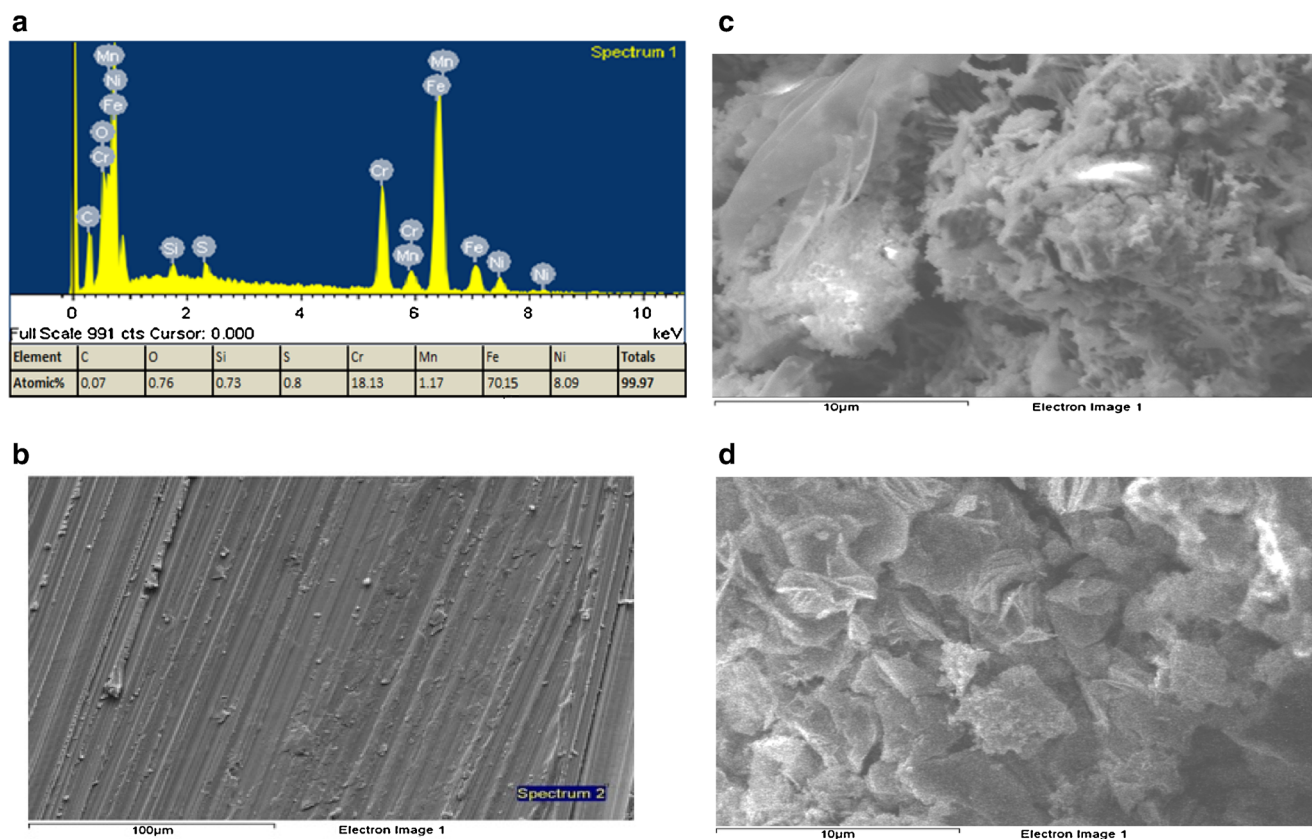
**Fig. 8** SEM micrographs of: (**a**) EDS analysis (**b**) Austenitic stainless steel, (**c**) Austenitic stainless steel in 3 M HCl, (**d**) Austenitic stainless steel in 3 M HCl with DMA

**Table 4** Identified Patterns List for XRD analysis of austenitic stainless steel in 3 M HCl without DMA

| Visible | Ref. Code | Score | Compound name | Displacement [° 2 Theta] | Scale factor | Chemical formula |
|---|---|---|---|---|---|---|
| * | 01-089-4185 | 51 | Iron | 0.312 | 0.497 | Fe |
| * | 00-048-0791 | 28 | Calcium Chromium Oxide | 0.7 | 0.058 | $Ca_2 Cr_2 O_5$ |
| * | 01-073-0603 | 41 | Hematite, syn | −0.187 | 0.032 | $Fe_2 O_3$ |

The presence of DMA in solution changes the surface topography of the steel in comparison to the uninhibited samples. The protective film efficiency is linearly proportional to the formation of a protective film with inhibiting power that increases with increase in DMA concentration as is visible in the micrographs. In Fig. 8d a continuous film is formed on the surface which cracked upon removal from the test solution. The specimen's surface from HCl solutions with DMA inhibitor is well protected, as the inhibitor molecules fully cover the metal surface, giving it a high degree of protection against corrosion. This indicates the formation of a superficial layer providing a very good passivation on the steel electrode, in the presence of DMA. It can be concluded that the protective adsorption film of DMA formed on the specimen surface exhibited good inhibition performance for the corrosion of type 304 stainless steel in the acid solutions and the observation is in good agreement with the weight loss and electrochemical experiments.

### 3.6 XRD Analysis

X-ray diffraction (XRD) patterns of the surface of the stainless steel samples in the acid test solutions gave qualitative information about the possible phases present. From Fig. 9 (a & b) the peaks at $2\theta = 50.5°$ and $39.5°$ for the steel in the absence of DMA indicate the presence of iron (iii) oxide ($Fe_2O_3$) formed due to corrosion on the steel. This is absent from the peaks in the presence of DMA in 3 M HCl. These observations clearly prove the influencing role of DMA on the corrosion protection of stainless steel (Tables 4 and 5).

### 3.7 Adsorption Isotherm

The mechanism of inhibition can be explained based on the interaction of the DMA with the metal surface. Adsorption isotherms enable the determination of the mechanism of metal-inhibitor interactions as a result of the bond formation between the inhibitor molecule and the metal. The Langmuir adsorption isotherm was applied to describe the adsorption mechanism for DMA in 3 M HCl solution, as it best fits the experimental results at 25 °C ambient temperature.

The conventional form of the Langmuir isotherm is,

$$\left[\frac{\theta}{1-\theta}\right] = K_{ads}C \tag{7}$$

and rearranging gives

$$\left[\frac{c}{\theta} = \frac{1}{\theta}\right] + C \tag{8}$$

where $\theta$ is the value of surface coverage on the steel alloy, $C$ is DMA concentration in the acid solution, and $K_{ads}$ is the equilibrium constant of the adsorption process. The plots of $\frac{c}{\theta}$ versus the inhibitor concentration $C$ are linear (Fig. 10) indicating Langmuir adsorption.

The deviation of the slopes from unity in Fig. 10 is attributed to the molecular interaction among the DMA molecules on the metal surface and changes in the values of the Gibbs free energy relative to the surface coverage.

Langmuir proposes the following;

(i) The molecular interaction between the inhibiting compounds on the metal surface is constant

(ii) The Gibbs free energy does not depend on the amount of surface coverage.

(iii) The effect of lateral interaction among the inhibiting compounds on the value of the Gibbs free energy is negligible [46]

The Langmuir isotherm predicts unity but the fitted values are less than unity for the slopes thereby indicating minimal deviation from the ideal conditions for the isotherm.

**Table 5** Identified Patterns List for XRD analysis of austenitic stainless steel in 3 M HCl with DMA

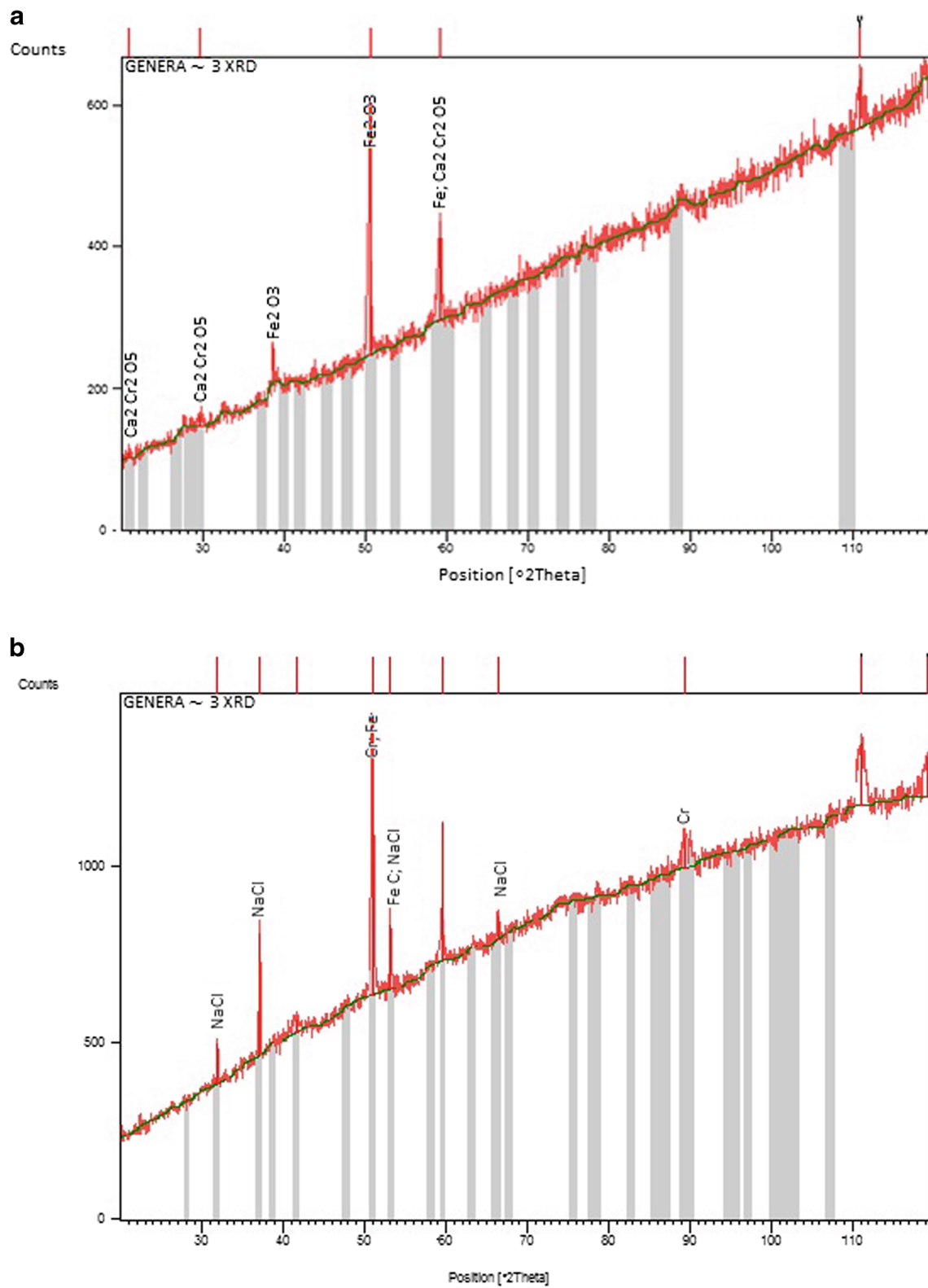| Visible | Ref. Code | Score | Compound name | Displacement [°2 Theta] | Scale factor | Chemical formula |
|---|---|---|---|---|---|---|
| * | 00-034-0396 | 30 | 434-L stainless steel | 0.881 | 0.258 | Fe - Cr |
| * | 01-088-2323 | 67 | Chromium | −0.045 | 0.99 | Cr |
| * | 01-078-0751 | 69 | Sodium Chloride | −0.324 | 0.394 | Na Cl |

**Fig. 9** XRD pattern of the surface film formed on austenitic stainless steel after immersion in 3 M HCl (**a**) without DMA (**b**) with DMA
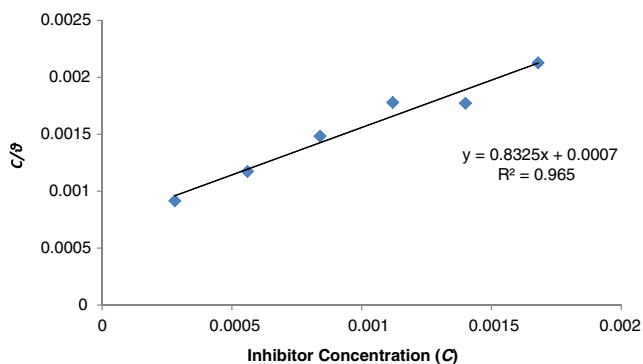
Fig. 10 Relationship between $\frac{c}{\theta}$ and inhibitor concentration (C) in 3 M HCl



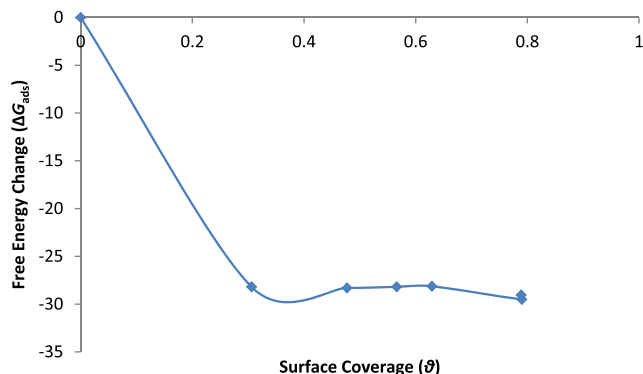Fig. 11 $\Delta G_{ads}$ on austenitic stainless steel as a function of surface coverage in 3 M HCl

## 3.8 Thermodynamics of the Corrosion Process

The values of the Gibbs free energy ($\Delta G_{ads}$) for the adsorption process can be evaluated from the equilibrium constant of adsorption using the following equation as shown in Table 6.

$$\Delta G_{ads} = -2.303RT \log[55.5K_{ads}] \quad (9)$$

Where 55.5 is the molar concentration of water in the solution, $R$ is the universal gas constant, $T$ is the absolute temperature and $K_{ads}$ is the equilibrium constant of adsorption. $K_{ads}$ is related to surface coverage ($\theta$) by the following equation.

$$K_{ads}C = \left[\frac{\theta}{1-\theta}\right] \quad (10)$$

The results presented in Table 6 provide additional evidence of slight deviation from ideal condition of the Langmuir model as observed in the different values of free energy of adsorption ($\Delta G_{ads}$) with increase in surface coverage ($\theta$) values. The relationship between $\Delta G_{ads}$ and $\theta$ is shown in Fig. 11. This suggests steric interactions between the adsorbed molecules on the surface.

The dependence of free energy of adsorption ($\Delta G_{ads}$) of DMA on surface coverage is a result of the inhomogeneous nature of the steel. On the stainless steel not all sites are equivalent on the surface, thus the different adsorption energies as observed in the experimental data (Table 6). The surface energy depends on surface properties of the metal and the flaws (such as dislocations, vacancies, microdistortions of crystal lattice, etc) on the surface. The value of $\Delta G_{ads}$ shows the capacity of DMA to strongly adsorb to the steel surface in HCl acid. The negative sign of $\Delta G_{ads}$ values shows that there was spontaneous adsorption of DMA molecules on the alloy surface. The values of $\Delta G_{ads}$ determined varied from between 28.13 kJ mol$^{-1}$ and 29.50 kJ mol$^{1}$ in HCl solutions. Values of $\Delta G_{ads}$ of about -20 kJ/mol or below align with weak molecular interaction and electrostatic attractions between the charged molecules and the charged metal and values around -40 kJ/mol or above involve the formation of a covalent type of bond [59, 60].

Accordingly, the value of $\Delta G_{ads}$ obtained in the present study indicates that the adsorption mechanism of DMA on austenitic stainless steel is physicochemical i.e. the combined action of electrostatic attraction and chemical reaction mechanism forms an insoluble protective film on the metal surface. This decreases the dissolution of metal. Acid anions due to the ionization affect the adsorption and degree of inhibition. The surface coverage of DMA is minimal when adsorption takes effect being adsorbed

Table 6 Results of Gibbs free energy, surface coverage and equilibrium constant of adsorption at specific concentrations of DMA in 3 M HCl

| Inhibitor Concentration (C) | Free energy of Adsorption ($\Delta G_{ads}$) (kJ/mol) | Surface coverage ($\theta$) | Equilibrium constant of adsorption ($K_{ads}$) |
|---|---|---|---|
| 0 | 0 | 0 | 0 |
| 0.00028 | −28.19 | 0.306 | 1572.7 |
| 0.00056 | −28.30 | 0.477 | 1629.1 |
| 0.00084 | −28.19 | 0.566 | 1552.2 |
| 0.00112 | −28.13 | 0.629 | 1515.2 |
| 0.00140 | −29.50 | 0.790 | 2679.8 |
| 0.00168 | −29.04 | 0.789 | 2228.4 |

**Table 7** Analysis of variance (ANOVA) for inhibition efficiency of DMA inhibitor in 3 M HCl (at 95 % confidence level)

| Source of variation | Sum of squares | Degree of freedom | Mean square | Mean square ratio | Min. MSR at 95 % confidence Significance $F$ | $F(\%)$ |
|---|---|---|---|---|---|---|
| Inhibitor concentration | 6932.96 | 5 | 1386.59 | 136.91 | 2.71 | 88.97 |
| Exposure time | 687.37 | 4 | 171.84 | 16.97 | 2.87 | 8.16 |
| Residual | 202.56 | 20 | 10.13 | | | |
| Total | 7822.89 | 29 | | | | |

to sites with the greatest bonding power electrostatically. The inhibitor first forms a protective film over the stainless steel through physisorption before being chemically bonded to the steel hence the variable values of $\Delta G_{\text{ads}}$.

### 3.9 Statistical Analysis

A two-factor single level statistical analysis using the ANOVA test ($F$-test) was used to determine the statistical significance of DMA concentration and exposure time on the inhibition efficiency values of the DMA in the acid solution. The $F$-test was applied to study the amount of variation within each of the samples relative to the amount of variation between the samples.

The Sum of squares among columns (exposure time) was obtained with Eq. 11.

$$SS_{\text{c}} = \frac{\Sigma T_{\text{c}^2}}{nr} - \frac{T^2}{N} \tag{11}$$

Sum of Squares among rows (inhibitor concentration)

$$SS_{\text{r}} = \frac{\Sigma T_{\text{r}}^2}{nr} - \frac{T^2}{N} \tag{12}$$

Total Sum of Squares

$$SS_{\text{Total}} = \Sigma \chi^2 - \frac{T^2}{N} \tag{13}$$

The results using the ANOVA test are shown in Table 7.
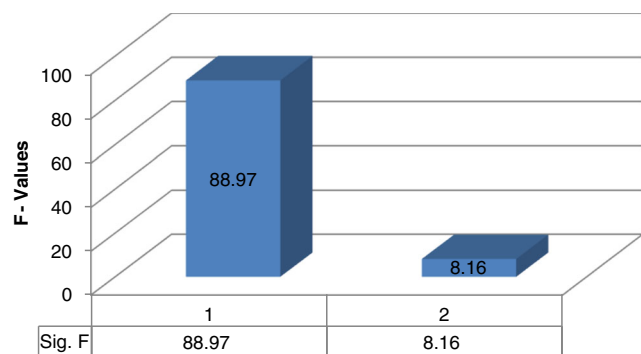


**Fig. 12** Influence of inhibitor concentration and exposure time on inhibition efficiency of DMA in 3 M HCl

The ANOVA analysis was evaluated for a confidence level of 95 % i.e. a significance level of $\alpha = 0.05$. The ANOVA results reveal that both experimental sources of variation (inhibitor concentration and exposure time) are statistically significant on the inhibition efficiency with $F$-values of 136.91 and 16.97 which are greater than the significance factor at $\alpha = 0.05$. The statistical influence of the inhibitor concentration is 88.97 % while the exposure time is 8.97 % depicting the overwhelming influence of inhibitor concentration on the values of inhibition efficiency from the experiments in comparison to the exposure time which is very small; however both are influential on the performance of DMA in 3 M HCl solution (Fig. 12).

## 4 Conclusion

2-dimethylaminoethanol showed excellent corrosion inhibition; effectively reducing the corrosion rate of austenitic stainless steel at the concentrations investigated from weight-loss, potential measurement and potentiodynamic polarization tests. The inhibition efficiency increased proportionately with increase in concentration of 2-dimethylaminoethanol as a result of the presence of more inhibitor molecules to stifle the corrosion process. Adsorption of 2-dimethylaminoethanol on the stainless steel surface fitted into the Langmuir model, thus indicating that the molecular interaction is fixed and the effect of lateral interaction among the adsorbates on the value of the Gibbs free energy is negligible. XRD analysis of the steel specimen surface showed diffraction peaks for the inhibited steel surfaces revealing the absence of iron oxides, chemical compounds and complexes associated with corrosion. At a confidence level of 95 % the ANOVA results in test solutions showed the overwhelming influence and statistical significance of inhibitor concentration over exposure time on the inhibition efficiency of 2-dimethylaminoethanol.

# References

1. Ariga K, Yamauchi Y, Rydzek G, Ji Q, Yonamine Y, Wu KCW, Hill JP (2014) Layer-by-layer nanoarchitectonics: invention, innovation, and evolution. Chem Lett 43:36–68

2. Matsumoto T, Sata N, Kobayashi K, Yamabe-Mitarai Y (2013) Surface structures and electrochemical activity of palladium–niobium binary alloy electrodes, and glucose biosensor with palladium–niobium binary alloy electrode. Bull Chem Soc Jpn 86:1317–1322

3. Bodhak S, Kikuchi M, Sogo Y, Tsurushima H, Ito A, Oyan A (2013) Calcium phosphate coating on a bioresorbable hydroxyapatite/collagen nanocomposite for surface functionalization. Chem Lett 42:1029–1031

4. Masuda K, Matsune H, Takenaka S, Kishida M (2014) Synthesis of silica-coated AgCl nanoparticles in aqueous poly(vinylpyrrolidone) solution. Bull Chem Soc Jpn 87:573–575

5. Singh DDN, Singh TB, Gaur B (1995) The role of metal cations in improving the inhibitive performance of hexamine on the corrosion of steel in hydrochloric acid solution. Corros Sci 37:1005–1019

6. Jayalakshmi M, Muralidharan VS (1998) Correlation between structure and inhibition of organic compounds for acid corrosion of transition metals. Ind J Chem Tech 5:16–28

7. Granese SL (1998) Study of the inhibitory action of nitrogen-containing compounds. Corrosion Corro J 44:322–329

8. Granese SL, Rosales BM, Oviedo C, Zebrino JO (1992) The inhibition action of heterocyclic nitrogen organic compounds on Fe and steel in HCl media. Corros Sci 33:1439–1453

9. Raicheva SN, Aleksiev BV, Sokolova EI (1993) The effect of the chemical structure of some nitrogen- and sulphur-containing organic compounds on their corrosion inhibiting action. Corros Sci 34:343–350

10. Frignani A, Monticelli C, Brunoro G, Zucchi M, Hashi OI (1987) Inhibitors for Armco iron and ASTM A106 plain steel in hydrofluoric acid. Brit Corr J 22:103–108

11. Cheng XL, Ma HY, Chen SH, Yu R, Chen X, Yao ZM (1999) Corrosion of stainless steels in acid solutions with organic sulfur-containing compounds. Corros Sci 41:321–333

12. El-Sayed A (1997) Phenothiazine as inhibitor of the corrosion of cadmium in acidic solutions. J Appl Electrochem 27:193–200

13. Schmitt G (1984) Application of inhibitors for acid media: report prepared for the European federation of corrosion working party on inhibitors. Brit Corr J 19:165–176

14. Abd El Rehim SS, Ibrahim MAM, Khalid KF (1999) 4-Aminoantipyrine as an inhibitor of mild steel corrosion in HCl solution. J Appl Electrochem 29:593–599

15. Hluchan V, Wheeler BL, Hackerman N (1988) Amino acids as corrosion inhibitors in hydrochloric acid solutions. Mats Corr 39(11):512–517

16. Behpour M, Ghoreishi SM, Soltani N, Salavati-Niasari M, Hamadanian M, Gandomi A (2008) Electrochemical and theoretical investigation on the corrosion inhibition of mild steel by thiosalicylaldehyde derivatives in hydrochloric acid solution. Corros Sci 50:2172–2188

17. Morad MS, Sarhan AAO (2008) Application of some ferrocene derivatives in the field of corrosion inhibition. Corros Sci 50:744–753

18. Khaled KF (2008) Magnetic properties of nanocomposite Fe-doped SBA-15 magnetic materials. Mats Chem Phys 112:290–300

19. Hosseini MG, Arshadi MR (2009) Study of 2-butyne-1,4-diol as acid corrosion inhibitor for mild steel with electrochemical, infrared and AFM techniques. Int J Electrochem Sci 4:1339–1350

20. Growcock FB, Lopp VR (1998) The inhibition of steel corrosion in hydrochloric acid with 3-phenyl-2-propyn-1-ol. Corros Sci 28:397–410

21. Tedeschi RJ (1975) Acetylenic corrosion inhibitors. Corros J 31:130–134

22. Yazdzad AR, Shahrabi T, Hosseini MG (2008) Inhibition of 3003 aluminum alloy corrosion by propargyl alcohol and tartrate ion and their synergistic effects in 0.5 % NaCl solution. Mat Chem Phy 109:199–205

23. Shahrabi T, Yazdzad AR, Hosseini MR (2008) Inhibition behaviour of 2-butine1, 4diol and tartrate salt, and their synergistic effects on corrosion of AA3003 aluminium alloy in 0.5 % NaCl solution. J Mat Sci Tech 24:427–432

24. Hosseini MG, Shahrabi T, Tavakholi HJ (2008) Synergism in copper corrosion inhibition by sodium dodecylbenzene-sulphonate and 2-mercaptobenzoimidazole. J Appl Elec 38:1629–1636

25. Paty BB, Singh DDN (1992) Solvents' role on HCl-induced corrosion of mild steel: its control by propargyl alcohol and metal cations. Corros J 48:442–527

26. Bartos M, Hackerman N (1992) A study of inhibition action of propargyl alcohol during anodic dissolution of iron in hydrochloric acid. J Electrochem Soc 139:3428–3433

27. Bilgiç S, Sahin M (2001) The corrosion inhibition of austenitic chromium–nickel steel in H2SO4 by 2-butyn-1-ol. Mat Chem Phy 70:290–295

28. Fontana MG, Staehle RW (1974) Plenum (Eds.), Advances in Corrosion Science and Technology, New York, pp 229

29. Putilova JN (1966) Comptes Rendus du 2eme. In: Symposium Europeen sur les Inhibiteurs de Corrosion, Annali University, Ferrara

30. Hosseini MG, Mertens SFL, Nichols RJ, Ghorbani M, Arshadi MR (2002) Eurocorr. Madrid, pp 24

31. Morris W, Vázquez M (2002) A migrating corrosion inhibitor evaluated in concrete containing various contents of admixed chlorides. Cem Concr Res 32:259–267

32. Elsener B, Büchler M, Stalder F, Böhni H (1999) Migrating corrosion inhibitor blend for reinforced concrete: part 1—prevention of corrosion. Corros J 55:1155–1163

33. Elsener B, Büchler M, Stalder F, Böhni H (2000) Migrating corrosion inhibitor blend for reinforced concrete: part 2—inhibitor as repair strategy. Corros J 56:727–732

34. Rosenberg A (2000) Discussion: migrating corrosion inhibitor blend for reinforcing concrete: part 1—prevention of corrosion. Corros J 56:986–987

35. Maeder U, Swamy RN (eds) (1994) Corrosion and corrosion protection of steel in concrete. Sheffield, U.K., p 851

36. Batis G, Routoulas A, Rakanta E (2003b) Effects of migrating inhibitors on corrosion of reinforcing steel covered with repair mortar. Cem Concr Compos 25:109–115

37. Jamil HE, Shriri A, Boulif R, Bastos C, Montemor MF, Ferreira MGS (2004) Electrochemical behaviour of amino alcohol-based inhibitors used to control corrosion of reinforcing steel. Electrochim Acta 49:2753–2760

38. Machnikova E, Kenton HW, Hackerman N (2008) Corrosion inhibition of carbon steel in hydrochloric acid by furan derivatives. Electroch Acta 53(20):6024–6032

39. Vaidyanathan H, Hackerman N (1971) Effect of furan derivatives on the anodic dissolution of Fe. Corros Sci 11:737–750

40. Moretti G, Guidi F, Grion G (2004) Tryptamine as a green iron corrosion inhibitor in 0.5 M deaerated sulphuric acid. Corros Sci 46:387–403

41. Oliveres O, Likhanova NV, Gomez B, Navarrete J, Llanos-Serrano ME, Arce E, Hallen JM (2006) Appl Surf Sci 252:2894–2909

42. Zhang DQ, Gao LX, Zhou GD (2003) Synergistic effect of 2-mercapto benzimidazole and KI on copper corrosion inhibition in aerated sulfuric acid solution. J Appl Electrochem 33:361–366

43. Oguzie EE, Unaegbu C, Ogukwe CN, Okolue BN, Onuchukwu AI (2004) Inhibition of mild steel corrosion in sulphuric acid using indigo dye and synergistic halide additives. Mater Chem Phys 84:363–368

44. Shibli SMA, Saji VS (2005) Co-inhibition characteristics of sodium tungstate with potassium iodate on mild steel corrosion. Corros Sci 47:2213–2224

45. Mu G, Li X (2005) Inhibition of cold rolled steel corrosion by Tween-20 in sulfuric acid: weight loss, electrochemical and AFM approaches. J Colloid Interface Sci 289: 184–192

46. Feng Y, Siow KS, Teo WK, Hsieh AK (1999) The synergistic effects of propargyl alcohol and potassium iodide on the inhibition of mild steel in 0.5 M sulfuric acid solution. Corros Sci 41:829–852

47. Villamil RFV, Corio P, Rubin JC, Agostinho SMI (1999) Effect of sodium dodecylsulfate on copper corrosion in sulfuric acid media in the absence and presence of benzotriazole. J Electroanal Chem 472:112–119

48. Wang B, Du M, Zhang J, Gao CJ (2011) Electrochemical and surface analysis studies on corrosion inhibition of Q235 steel by imidazoline derivative against CO2 corrosion. Corros Sci 53:353–361

49. Brett CMA, Gomes IAR, Martins JPS (1994) The electrochemical behaviour and corrosion of aluminium in chloride media. The effect of inhibitor anions. Corros Sci 36:915–923

50. Olivares O, Likhanova NV, Gomez B, Navarrete J, Llanos-Serrano ME, Arce E, Hallen JM (2006) Electrochemical and XPS studies of decylamides of a-amino acids adsorption on carbon steel in acidic environment. Appl Surf Sci 252:2894–2909

51. Trasatti S (1992) Adsorption of organic substances at electrodes: recent advances. Electrochim Acta 37:2137–2144

52. Popova A, Sokolova E, Raicheva S, Christov M (2003) AC and DC study of the temperature effect on mild steel corrosion in acid media in the presence of benzimidazole derivatives. Corros Sci 45:33–58

53. Revie RW (2000) Uhlig's corrosion handbook. Wiley, New York

54. Altsybeeva AI, Burlov VV, Fedorova NS, Reshetnikov SM (2013) Volatile inhibitors of atmospheric corrosion of ferrous and nonferrous metals. V. Study of the adsorption of inhibitors on steel from an aqueous electrolyte solution. Int J Corros Scale Inhib 2(4):277–286

55. Yasser K, Mohammed El AB, Ali D, Belkheir H (2014) A theoretical investigation on the corrosion inhibition of mild steel by piperidine derivatives in hydrochloric acid solution. J of Chem Pharm Research 6(4):689–696

56. Amitha RBE, Bharathi Bai JB (2012) Green inhibitors for corrosion protection of metals and alloys: an overview. Int J of Corrosion. doi:10.1155/2012/380217

57. Noor EA, Al-Moubaraki AH (2008) Thermodynamic study of metal corrosion and inhibitor adsorption processes in mild steel/1-methyl-4[4′(-X)-styryl pyridinium iodides/hydrochloric acid systems. Mats Chem Phys 110(1):145–154

58. Aljourani J, Raeissi K, Golozar MA (2009) Benzimidazole and its derivatives as corrosion inhibitors for mild steel in 1 M HCl solution. Corros Sci 51(8):1836–1843

59. Obot B, Obi-Egbedi NO, Umoren SA (2009) Experimental and theoretical investigation of clotrimazole as corrosion inhibitor for aluminium in hydrochloric acid and effect of iodide ion addition. Der Pharm Chem 1:151–166

60. Hosseini MG, Mertens SFL, Arshadi MR (2009) Synergism and antagonism in mild steel corrosion inhibition by sodium dodecylbenzenesulphonate and hexamethylenetetramine. Corros Sci 45:1473–1489